

**PROCEEDINGS**

**SECOND INTERNATIONAL CONFERENCE ON INVERSE  
DESIGN CONCEPTS AND OPTIMIZATION  
IN ENGINEERING SCIENCES  
ICIDES-II**

October 26-28, 1987  
Penn State University  
University Park, Pennsylvania, U.S.A.

**Sponsored by:**

**OFFICE OF NAVAL RESEARCH**  
Department of the Navy  
Fluid Mechanics Division  
800 North Quincy Street  
Arlington, VA 222171

**NATIONAL SCIENCE FOUNDATION**  
Emerging Engineering Systems  
Computational Engineering  
180 G. Street, N.W.  
Washington, DC 20550

**PENN STATE UNIVERSITY**  
Aerospace Engineering Department  
233 Hammond Building  
University Park, PA 16802, U.S.A.

**Edited by: George S. Dulikravich**



The second problem will be addressed in this paper. An inverse design/optimization procedure will be presented that numerically determines the external temperature-time history that will minimize the destruction of living cells during the preservation process. The idea of using Boundary Element Method (BEM) in conjunction with optimization procedures was originated by Kennon and Dulikravich [3]. A conceptual steady state formulation using an iterative process adapted to the problem of cryo-preservation procedures was presented by Hayes, Dulikravich, and Chiang [4].

In this paper we will develop a physically time-dependent formulation using similar methods. The method is developed so that three separate regions with varying values of thermal diffusivity can be specified. The optimum cooling container wall temperatures will be determined at each time step by solving the time-dependent two-dimensional temperature diffusion equation using the boundary element method (Figure 1).

#### MATHEMATICAL FORMULATION

The governing equation for a two-dimensional time dependent heat conduction problem is given by

$$\kappa \Delta^2 T = \frac{\partial T}{\partial t} \quad \text{in } \Omega \times T \quad (1)$$

subject to initial condition  $T(x, t_0) = T_0(x)$ , where  $T$  is the temperature,  $t$  is the time, and  $\kappa$  is the thermal diffusivity,  $\kappa = \lambda/\rho C$ . Here,  $\lambda$  is the heat conductivity,  $\rho$  is the material density and  $C$  is the specific heat capacity. All coefficients are assumed to be constant.

A Dirichlet type boundary condition ( $T = T_s$ ) can be applied on the part of the boundary ( $\Gamma_1$ ) and Neumann type boundary condition ( $\partial T/\partial n = q_s$ ), where  $n$  is the direction normal to the boundary, can be applied on the remaining part ( $\Gamma_2$ ) of the overall boundary ( $\Gamma = \Gamma_1 + \Gamma_2$ ).

For our numerical solution we will use a Boundary Element Method (BEM) formulation and the error will be reduced by weighting the governing equation by a new function  $T^*$ . This function is known as the fundamental solution of (1) and it is given [5] as

$$T^* = \frac{1}{4\pi\kappa(t-\tau)} \exp\left[-\frac{r}{4\kappa(t-\tau)}\right] \quad (2)$$

where  $r$  is the distance from the heat source point to the point under consideration,  $t$  is the final time, and  $\tau$  is the current time. Taking the normal derivative of (2) results in

$$q^* = \frac{\partial T^*}{\partial n} = -\frac{r}{8\pi\kappa^2(t-\tau)^2} \exp\left[-\frac{r}{4\kappa(t-\tau)}\right] \quad (3)$$

Integrating (1) with this weighting function gives [6]

$$\int_0^t \int_{\Omega} (\Delta^2 T - \frac{\partial T}{\partial t}) T^* d\Omega d\tau = \int_0^t \int_{\Gamma_2} (q - q_g) T^* d\Gamma d\tau - \int_0^t \int_{\Gamma_1} (T - T_g) q^* d\Gamma d\tau \quad (4)$$

where  $0 \leq \tau \leq t$ . Integrating by parts twice yields

$$\int_0^t \int_{\Omega} (\Delta^2 T^* + \frac{\partial T^*}{\partial t}) T d\Omega d\tau - \left[ \int_{\Omega} T T^* d\Omega \right]_{\tau=0}^{\tau=t} + \int_0^t \int_{\Gamma} q T^* d\Gamma d\tau = \int_0^t \int_{\Gamma} T q^* d\Gamma d\tau \quad (5)$$

The fundamental solution satisfies

$$\Delta^2 T^* + \frac{\partial T^*}{\partial t} = 0 \quad (6)$$

on domain  $\Omega$  for all  $\tau$ . For  $\tau = t$  it follows that

$$\int_{\Omega} T T^* d\Omega = \begin{cases} 0 & \text{for } \tau \neq 0 \\ 1 & \text{for } \tau = 0 \end{cases} \quad (7)$$

Substituting this solution into (5), it follows that at a point 'i' [6]

$$c_i T_i + \int_0^t \int_{\Gamma} T q^* d\Gamma d\tau = \int_0^t \int_{\Gamma} q T^* d\Gamma d\tau + \left[ \int_{\Omega} T T^* d\Omega \right]_{\tau=0} \quad (8)$$

The final term in (8) corresponds to the initial conditions at time  $\tau = 0$ . The coefficient  $c_i$  is the scaled internal angle, which is equal to 0.5 for a smooth point on the boundary, and equals 1.0 for a point in the interior of the domain [7]. In order to simplify the notation, a new set of operators will now be defined as

$$H = c + \int_0^t \int_{\Gamma} q^* d\Gamma d\tau \quad (9)$$

$$G = \int_0^t \int_{\Gamma} T^* d\Gamma d\tau \quad (10)$$

$$B = \left[ \int_0^t T T^* d\Omega \right]_{\tau=0} \quad (11)$$

Thus, (8) can now be written in vector operator form as

$$[H] \{T\} - [G] \{q\} = \{B\} \quad (12)$$

To evaluate (12) numerically, the boundary of the domain can be divided into elements, and a variation in time for the functions  $T$  and  $q$  must be assumed. Since these functions vary in time much slower than  $T^*$  and  $q^*$ , it is reasonable to assume that they are constant over small intervals of time, thus allowing us to perform the time integrations stepwise [8]. Hence, the integrals over time can be found analytically. The space integrals are more complicated and must be evaluated numerically. For this paper, the boundary integrals were calculated using a four point Gaussian quadrature. The integral over the domain is performed by discretizing it into triangular elements [9] and using a seven point quadrature by Hammer [10]. After each time step, the temperature at the internal nodes was calculated and used as the initial condition for the next time step.

For the case of spatially varying material properties, we have decided to divide the domain into separate subdomains, each having a different value for the thermal diffusivity,  $\kappa$ . The temperature and heat flux values along the common boundaries cannot be solved for directly. Instead, temperature and heat flux continuity conditions between the subdomains must be enforced to form the necessary additional equations. To implement this, the temperatures along each common boundary are enforced to be equal, and the heat flux values are enforced to be equal in magnitude but opposite in direction with respect to the outward normal of the boundary [7]. In this manner the system of equations for each subregion can be coupled to form one global system of equations which will yield the unknown temperature and heat flux quantities.

#### THE OPTIMIZATION PROCEDURE

For the case being considered, assume that the size and geometry of the transplant organ remains fixed and that the temperature on the cooling container wall can be continuously adjusted in order to maintain the specified cooling rate in the interior of the object. To implement this in time, one may assume the circumferential variation of temperature on the external circular boundary to be a polynomial of the form [4]

$$T = \alpha_0 + \alpha_1 \theta + \alpha_2 \theta^2 + \alpha_3 \theta^3 + \alpha_4 \theta^4 \quad (13)$$

where  $0 \leq \theta < 2\pi$  is the angle measured in the counter-clockwise direction.

Then, the coefficients of this polynomial could be adjusted iteratively in order to maintain the desired cooling rates. The initial values of the coefficients  $\alpha$  are guessed and the transient temperature distribution is found. From this, the calculated heat flux  $q_c$  is determined at each point in the interior. The desired values of temperature derivative with respect to time at each point are defined as  $\partial T_g / \partial t$ . A normalized error function can then be

defined in a least squares sense as [10]

$$E_0 = \frac{(1-\omega) \left[ \sum_{j=1}^N (T_c^j - T_s^j)^2 \right]^{1/2} + \omega \left[ \sum_{j=1}^N \left( \frac{\partial T_c^j}{\partial t} - \frac{\partial T_s^j}{\partial t} \right)^2 \right]^{1/2}}{\left[ \sum_{j=1}^N (T_s^j)^2 \right]^{1/2} + \left[ \sum_{j=1}^N \left( \frac{\partial T_s^j}{\partial t} \right)^2 \right]^{1/2}} \quad (14)$$

where  $0 \leq \omega \leq 1$  is the linear input weighting parameter.

The Davidson-Fletcher-Powell (DFP) function minimization method [11] is then used to compute new values of the coefficients  $\alpha$  in order to reduce the error at the next time step during the optimization process. The DFP method uses one-dimensional search directions and optimal step lengths in order to move towards the global minimum [12].

## RESULTS

In order to test the accuracy of the computer code that we developed, a test case with a known analytic solution was chosen first. This test case represents an annular region between two concentric circles of radii  $r_a = 1.0$  and  $r_b = 2.0$ . The initial temperature is given as  $T(r,0) = 1.0$  and the boundary conditions imposed are  $T(r_b,t) = 0.0$  and  $T(r_a,t) = 0.0$ . The analytic solution governing the space-time evolution of the temperature is given in terms of Bessel functions [5]

$$T(r,t) = \pi \sum_{n=1}^{\infty} \exp[-\kappa \alpha_n^2 t] \frac{J_0(a \alpha_n) [J_0(r \alpha_n) Y_0(b \alpha_n) - J_0(b \alpha_n) Y_0(r \alpha_n)]}{J_0(a \alpha_n) + J_0(b \alpha_n)} \quad (15)$$

where the roots are found from the equation

$$J_0(a \alpha_n) Y_0(b \alpha_n) - J_0(b \alpha_n) Y_0(a \alpha_n) = 0 \quad (16)$$

The annular domain was discretized with the nonstructured [9] computational grid (Figure 2) consisting of 194 triangles, each containing seven integration points. We used up to forty terms in the Bessel series to construct the exact solution at every time level. Nevertheless, at  $t = 0$  the Bessel series form of the analytic solution did not succeed in giving accurate values (Figure 3). At consequent time levels, a very good agreement between BEM without optimization and the analytic solution was obtained (Figure 4).

An actual kidney shape [13] configuration (Fig. 1) was approximated as a composite domain consisting of three concentric circles (Figure 5) each having different constant value of the diffusivity [14]. The most outer annular domain (Figure 6) simulated the kidney coolant domain, while the inner annulus (Figure 7) and the central solid circle (Figure 8) simulated two distinct tissues of an actual kidney. The constant diffusivity coefficients that we used were  $\kappa_1 = 0.145$ ,  $\kappa_2 = 0.169$ , and  $\kappa_3 = 0.255\text{cm}^2\text{s}^{-1}$  and represent values that are hundred times larger than the actual quantities [13].

Uniform initial temperature was  $T = 100^\circ\text{C}$  and the optimal cooling rate was enforced to be  $\partial T/\partial t = 5^\circ\text{C}/\text{sec}$ . Constant temperature contours (isotherms) for the optimized cooling of this test case are shown in Figures 9a-9g at equal time intervals  $\Delta t = 2\text{s}$ . Corresponding circumferential optimized wall temperature distributions are shown in Figure 10.

## CONCLUSIONS

Analysis capability of our code to predict rapid cooling (or warming) of complex configurations has been proven by comparing it to known analytic solutions. Inverse problem of specifying a desired cooling rate and finding the corresponding instantaneous temperature distribution on the wall of the cooling container has been proven to be feasible with the use of an optimization algorithm. Future research efforts will include temperature dependent diffusivities [15], latent heat effects [2], and three-dimensional reformulation of the problem. The entire concept remains to be verified experimentally.

## ACKNOWLEDGMENTS

The authors are grateful to Dr. Stephen R. Kennon for providing them with his nonstructured grid generation program. Mr. Steven Bova, Mr. Daniel Dorney, Mr. Alfred Lorber, and Mr. Jonathan Weiss helped us with computer networking and graphics and Ms. Amy Myers typed the final version of this article. The computing was performed on Apple and Sun computers donated to Penn State University Interdisciplinary Computational Fluid Dynamics Laboratory.

## REFERENCES

1. Mazur, P., "Cryobiology: The freezing of Biological Systems," Science, Vol. 168, 1970, pp. 939-949.
2. Hayes, L. J., Diller, K. R., and Crawford, M. E., "The Influence of Local Temperature History During Freezing of Impure Solutions on the Kinetics of Thermally Coupled Processes," ASME Paper #85-WA/HT-82, presented at the ASME Winter Annual Meeting, Miami Beach, Fl., Nov. 17-21, 1985.
3. Kennon, S. R. and Dulikravich, G. S., "The Inverse Design of Internally Cooled Turbine Blades," ASME PAPER 84-GT-7, presented at 29<sup>th</sup> Int'l Gas Turbine Conf., Amsterdam, The Netherlands, June 4-7, 1984.
4. Hayes, L. J., Dulikravich, G. S., and Chiang, T. L., "Inverse Design and Optimization of the Cryopreservation Process," Heat & Mass Transfer in Biomedical Systems Paper #34, presented at the 2<sup>nd</sup> Joint ASME-JSME Thermal Engineering Conference, Honolulu, HI, March 1987.

5. Carslaw, H. S. and Jeager, J. C., Conduction of Heat in Solids, 2nd Ed., Clarendon Press, Oxford, 1959.
6. Brebbia, C. A. and Wrobel, L. C., "Steady and Unsteady Potential Problems Using the Boundary Element Method," Recent Advances In Numerical Methods In Fluids, Vol. 1, Pineridge Press Ltd, Swansea, U. K., 1980.
7. Brebbia, C. A., et al., Boundary Element Techniques, Springer-Verlag, Berlin, Leidelberg, 1984.
8. Pena, H. L. G. and Fernandes, J. L. M., "Applications in Transient Heat Conduction," Topics in Boundary Element Research, Vol. 1: Basic Principles and Applications, Ed. by C. A. Brebbia, Springer-Verlag, New York, 1984.
9. Kennon, S. R., "Numerical Solution of Weak Forms of Conservation Laws on Optimal Unstructured Triangular Grids," Ph.D. Dissertation, Dept. of Aero. Eng. and Eng. Mech., Univ. of Texas at Austin, August 1987.
10. Segerlind, L. J., Applied Finite Element Analysis, 2nd Ed. Wiley and Sons, New York, 1984.
11. Chiang, T. L., "Inverse Design of Composite Multiholed Internally Cooled Turbine Blades," M. Sc. Thesis, Dept. of Aerospace Eng. and Eng. Mechanics, The University of Texas at Austin, Dec. 1985.
12. Luenberger, D. G., Linear and Nonlinear Programming, 2nd Ed., Addison-Wesley, New York, 1984.
13. Hayes, L. J. and Diller, K. R., "A Finite Element Model for Kidney Cooling, Including the Measurement and Numerical Effects of Differential Tissue Thermal Properties," Cryo-Letters Paper #137-148 (1983), Cryo-Letters, Cambridge.
14. Chiang, T. L., Dulikravich, G. S., and Hayes, L. J., "Inverse Design of Coolant Flow Passages in Ceramically Coated Scram Jet Combustor Struts," ASME-WAM Paper #33, presented at the special session of Numerical Methods in Heat Transfer, Anaheim, CA, Dec. 1986.
15. Kikuta, M. and Togoh, H., "Boundary Element Analysis of Nonlinear Transient Heat Conduction Problems," Comp. Meth. in Appl. Mech. and Eng., 62, 1987, pp. 321-329.





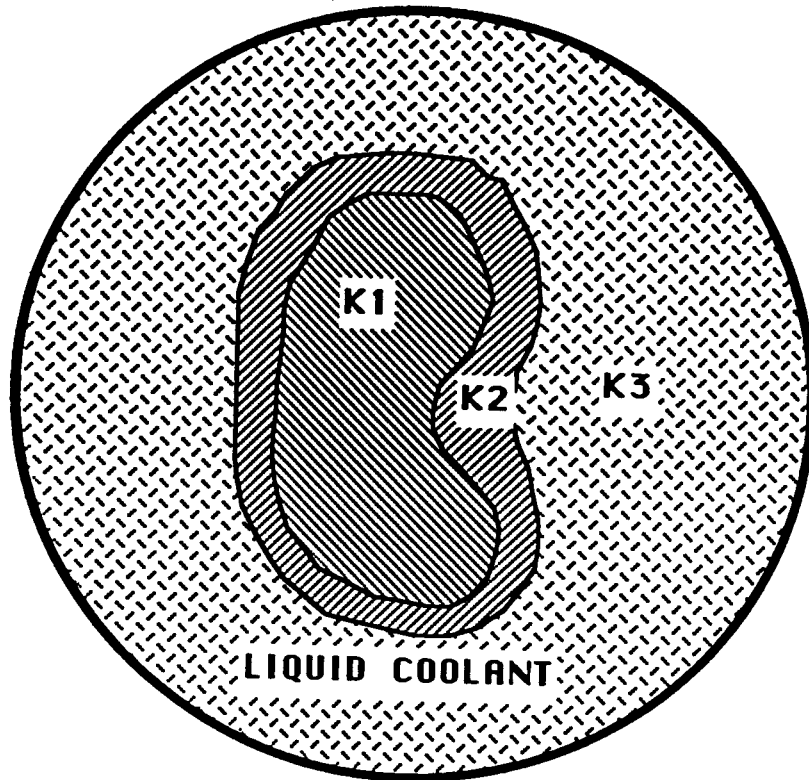


Figure 1. A Sketch of a Kidney Immersed in a Coolant Contained Within a Cylindrical Container

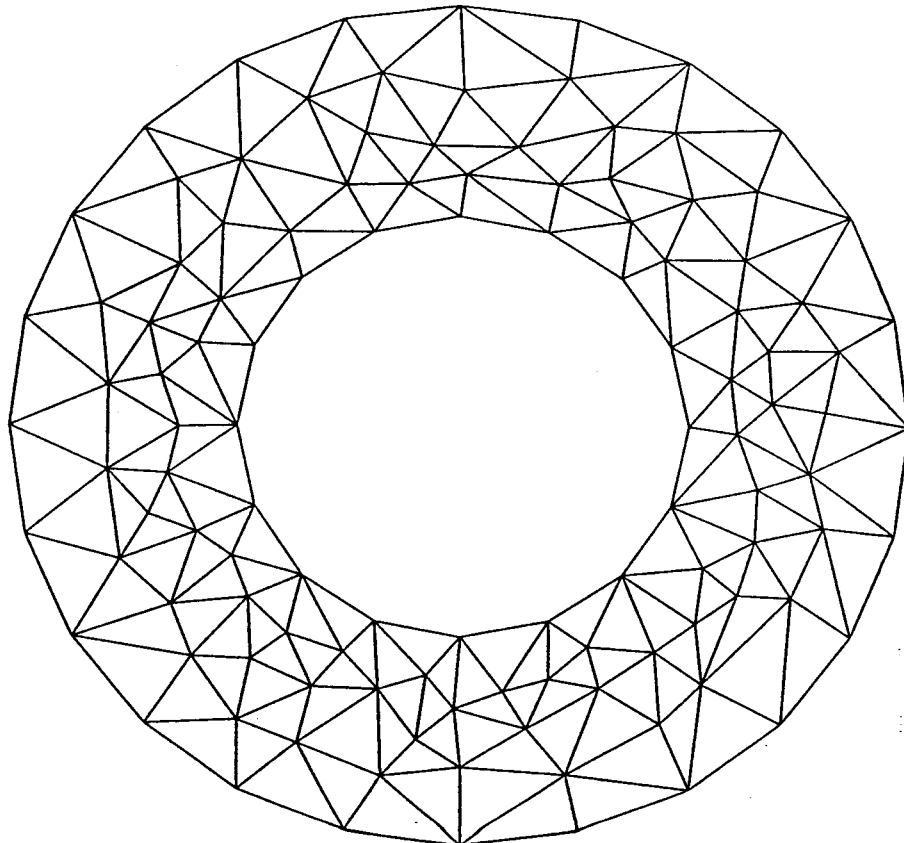


Figure 2. Analysis Case: Nonstructured Computational Grid for Annular Region

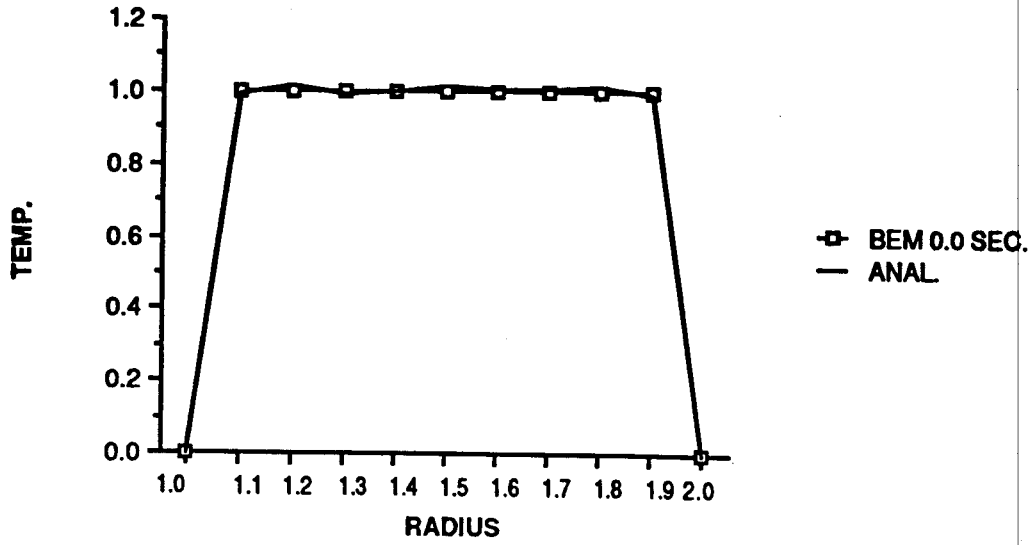


Figure 3. Analysis Case: Initial Temperature

Distribution    BEM; \_\_\_\_\_  
analytical

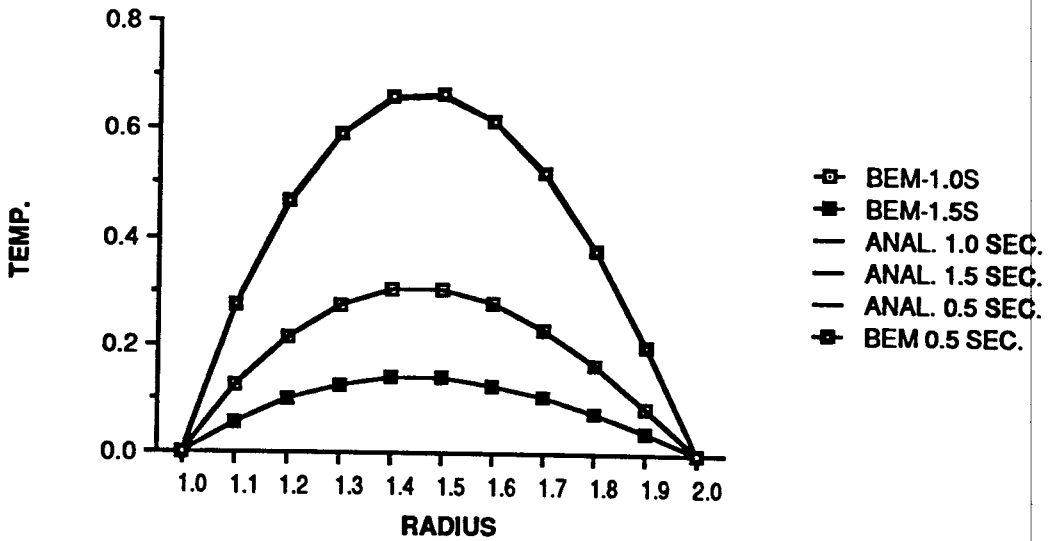


Figure 4. Analysis Case: Radial Temperature Distribution

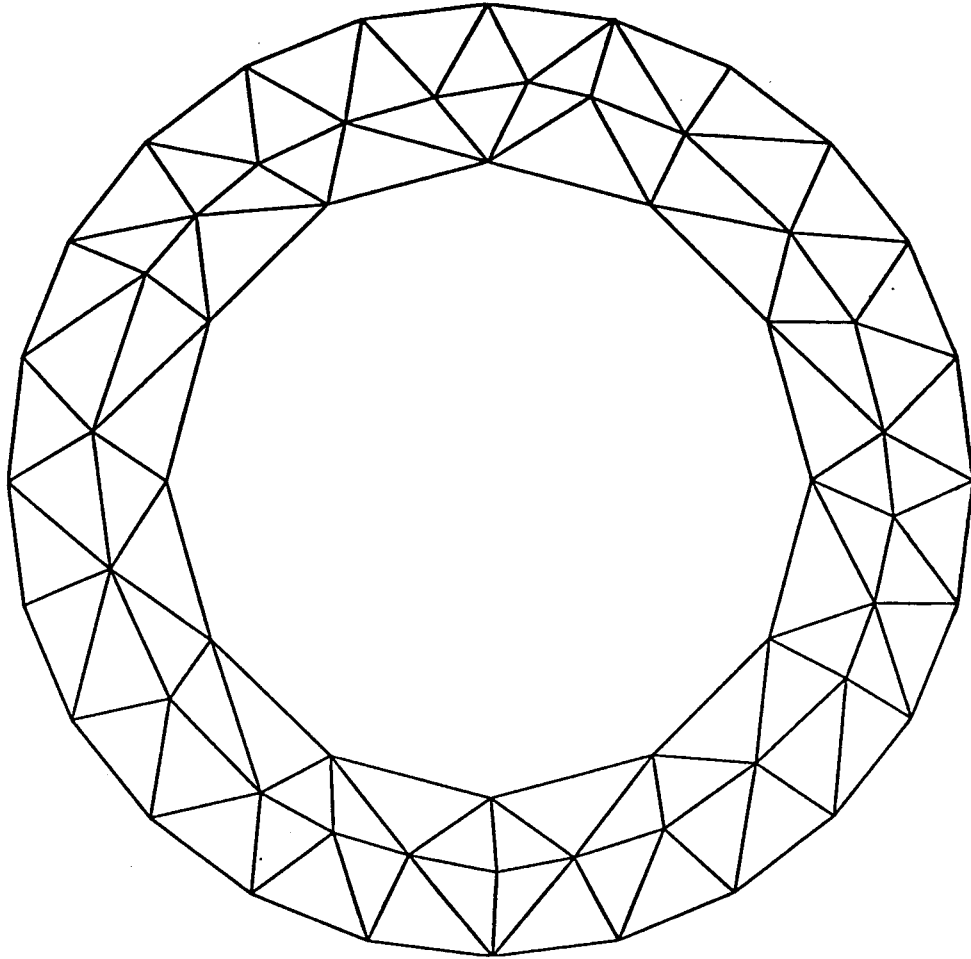


Figure 5. Nonstructured Grid for the Optimized Cooling Test Case : Outer Annular Region

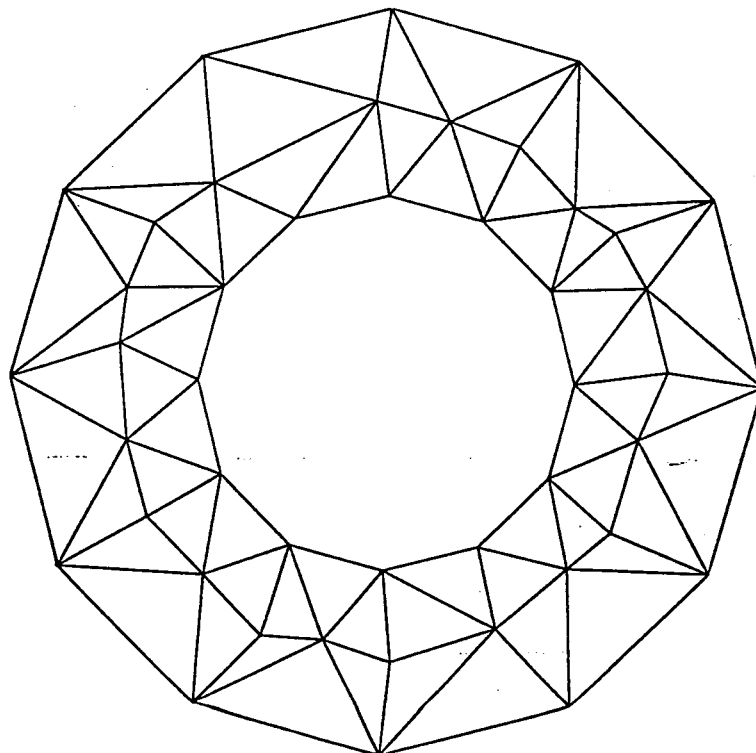


Figure 6. Nonstructured Grid for the Optimized Cooling Test Case : Inner Annular Region

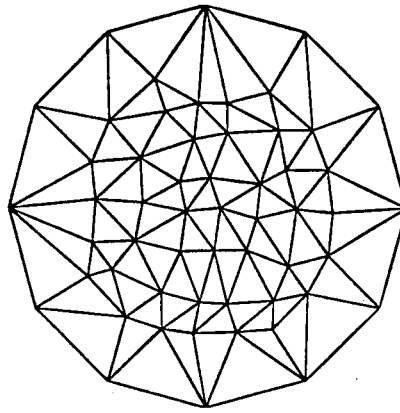


Figure 7. Nonstructured Grid for the Optimized Cooling Test Case : Central Circular Region

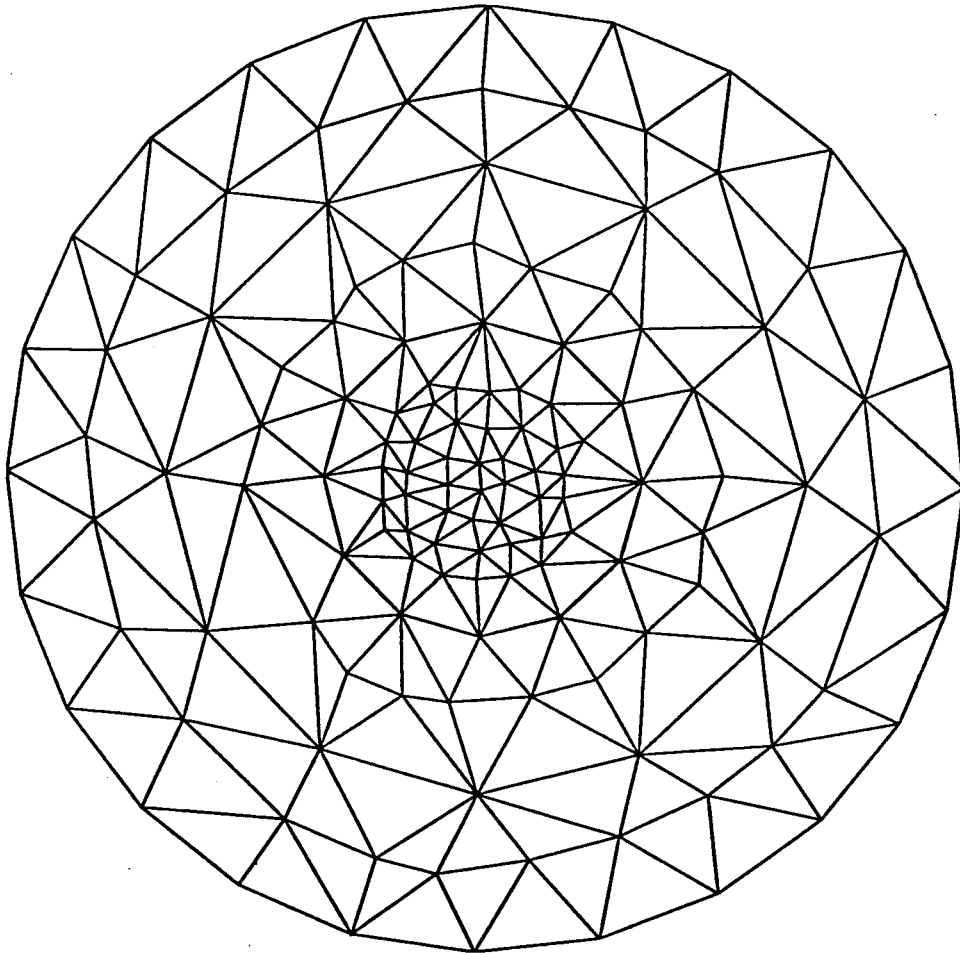


Figure 8. Nonstructured Grid for the Optimized Cooling Test Case : Composite Grid

0.8200  
0.8400  
0.8600  
0.8800  
0.9000  
0.9200  
0.9400  
0.9600  
0.9800

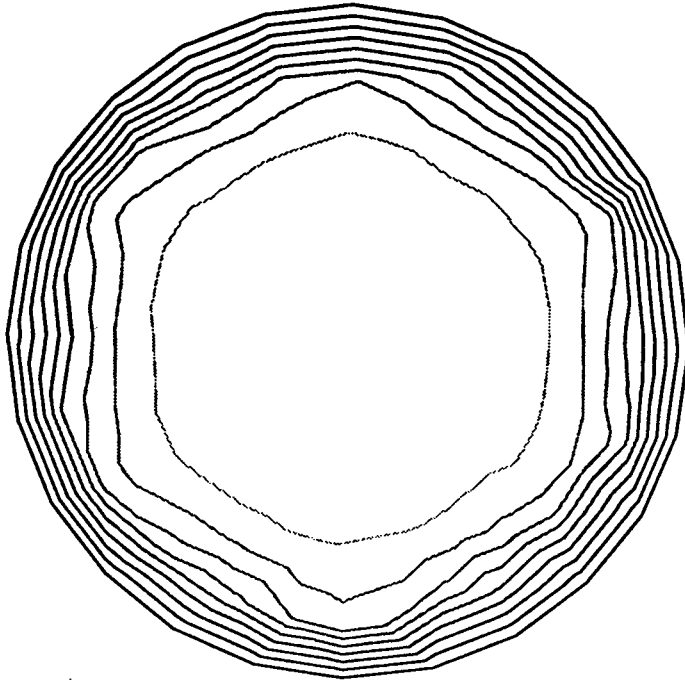


Figure 9a. Optimized Cooling Test Case:  
Isotherms After  $t = 2$  sec.

0.7600  
0.7800  
0.8000  
0.8200  
0.8400  
0.8600  
0.8800  
0.9000  
0.9200  
0.9400  
0.9600  
0.9800

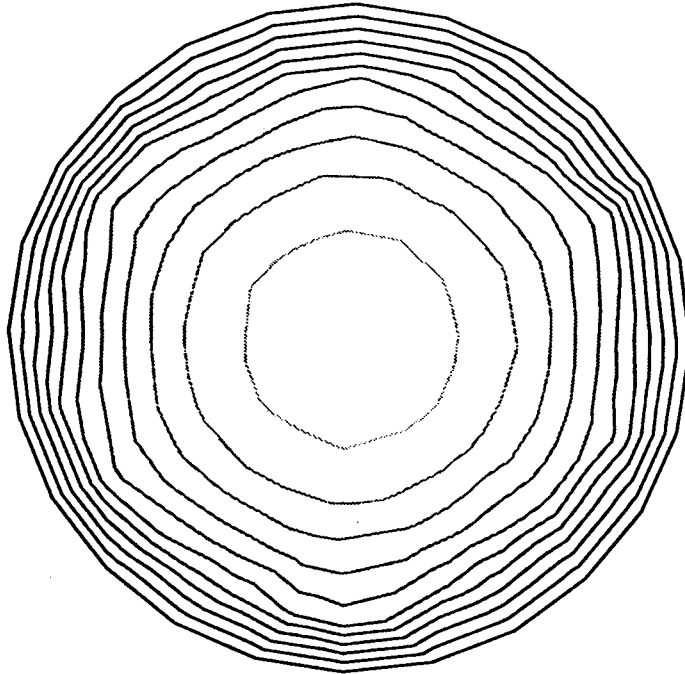


Figure 9b. Optimized Cooling Test Case:  
Isotherms After  $t = 4$  sec.

0.7000  
 0.7200  
 0.7400  
 0.7600  
 0.7800  
 0.8000  
 0.8200  
 0.8400  
 0.8600  
 0.8800  
 0.9000  
 0.9200  
 0.9400  
 0.9600  
 0.9800

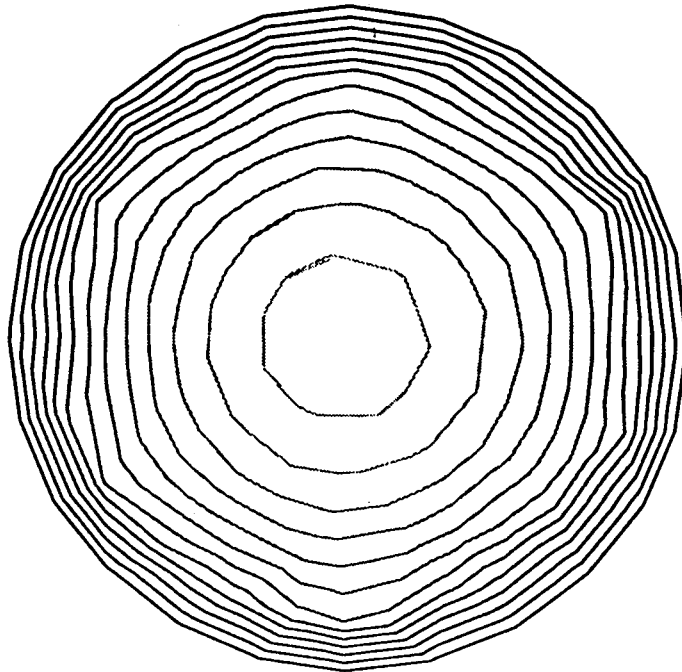


Figure 9c. Optimized Cooling Test Case:  
Isotherms After  $t = 6$  sec.

0.6400  
 0.6600  
 0.6800  
 0.7000  
 0.7200  
 0.7400  
 0.7600  
 0.7800  
 0.8000  
 0.8200  
 0.8400  
 0.8600  
 0.8800  
 0.9000

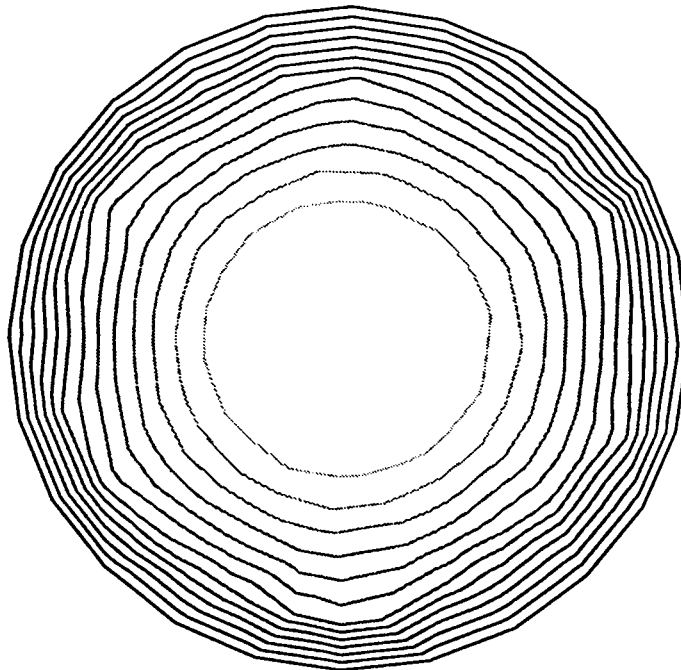


Figure 9d. Optimized Cooling Test Case:  
Isotherms After  $t = 8$  sec.

0.5800  
0.6000  
0.6200  
0.6400  
0.6600  
0.6800  
0.7000  
0.7200  
0.7400  
0.7600  
0.7800  
0.8000  
0.8200  
0.8400  
0.8600  
0.8800  
0.9000  
0.9200

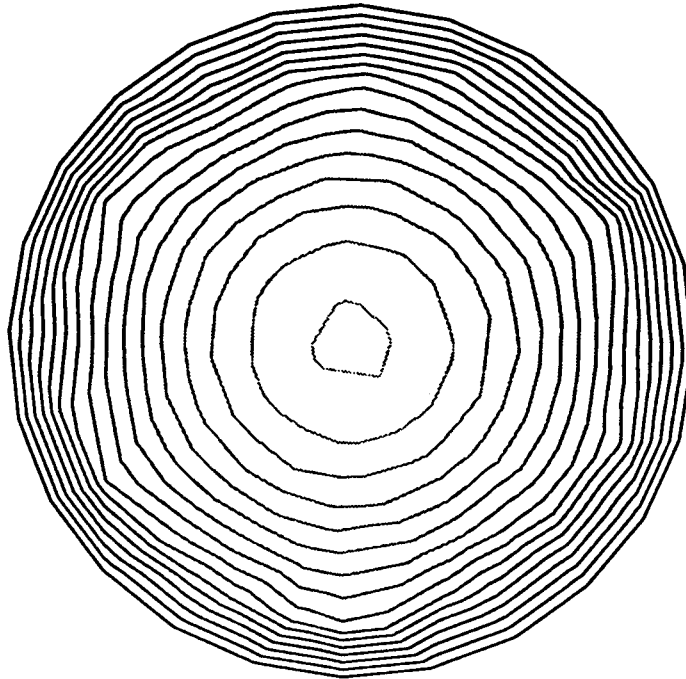


Figure 9e. Optimized Cooling Test Case:  
Isotherms After  $t = 10$  sec.

0.5400  
0.5600  
0.5800  
0.6000  
0.6200  
0.6400  
0.6600  
0.6800  
0.7000  
0.7200  
0.7400  
0.7600  
0.7800  
0.8000  
0.8200  
0.8400  
0.8600  
0.8800  
0.9000  
0.9200

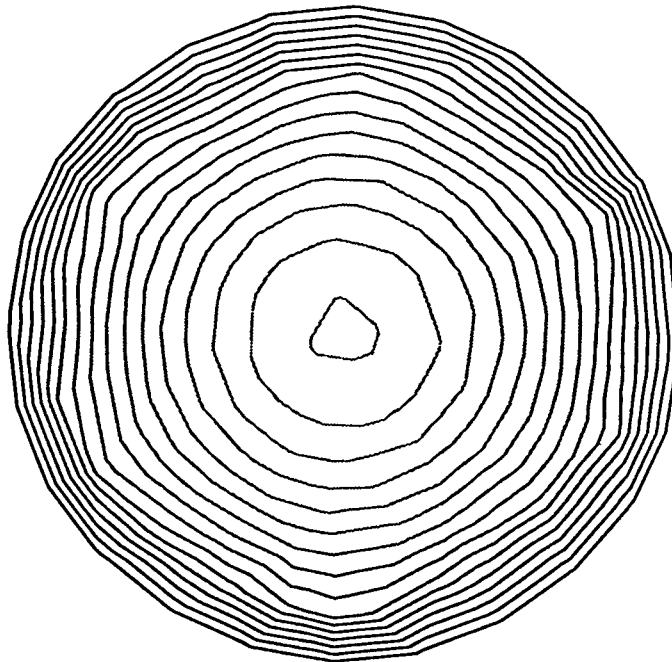


Figure 9f. Optimized Cooling Test Case:  
Isotherms After  $t = 12$  sec.



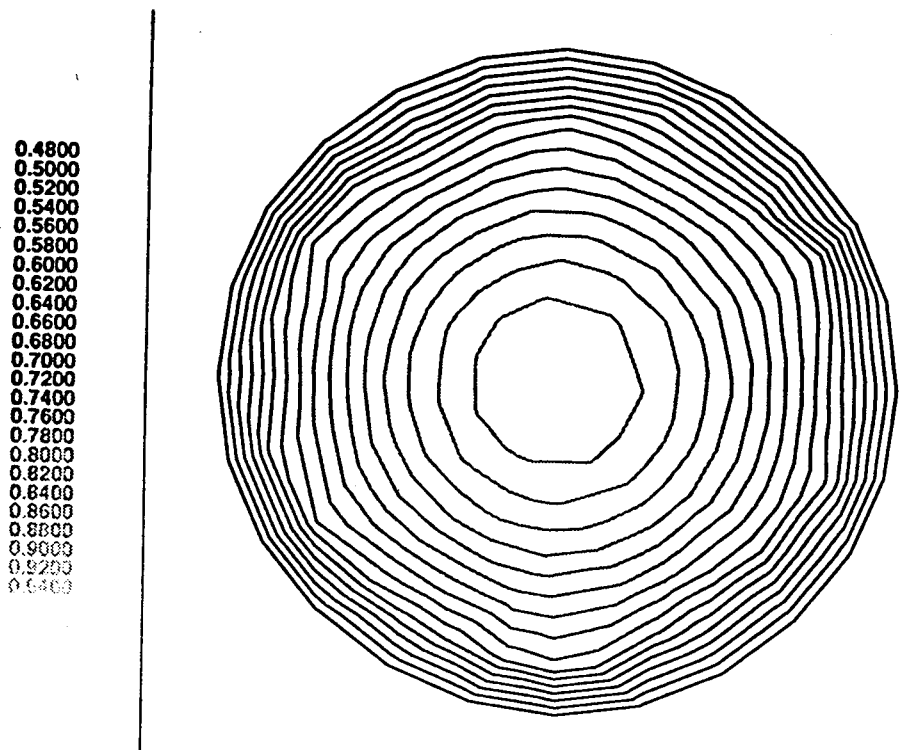


Figure 9g. Optimized Cooling Test Case:  
 Isotherms After  $t = 14$  sec.

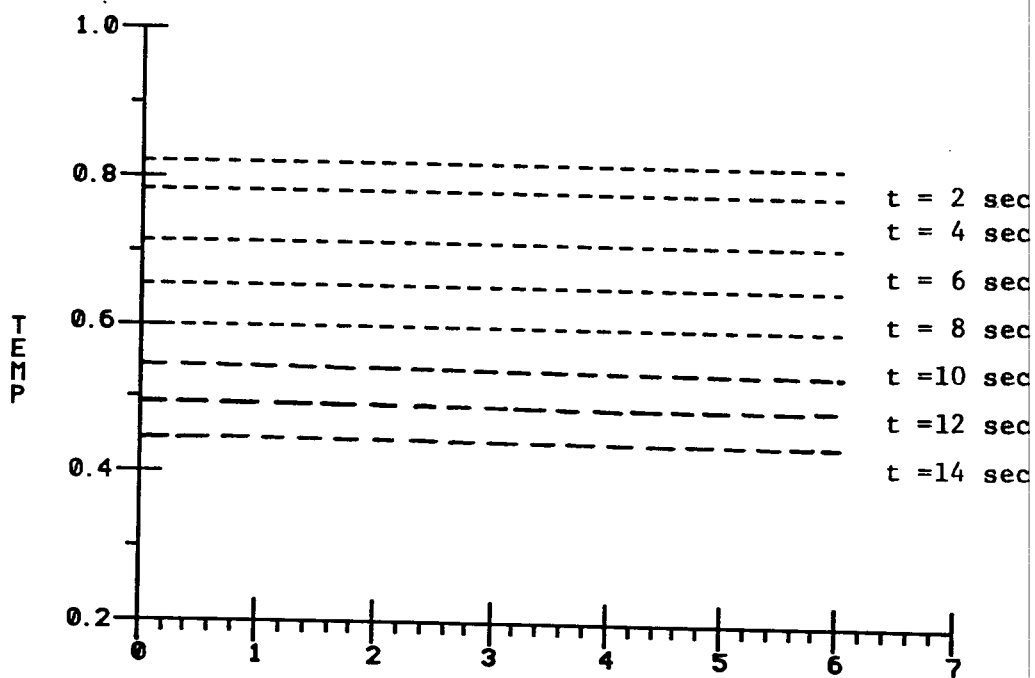


Figure 10. Optimized Container Wall Temperature  
 Variation With Respect to Time and  
 Angular position